Proceedings of the 12th International Forum of Automotive Traffic Safety, 2015, pp 221- 229
No. ATS.2015.S3A10

Optimization of Planing style energy absorbing anti-climbing device for crashworthiness designs based on Response surface method

Shiming Wang, Yong Peng, Ping XU, Zhiqun Yuan
Key Laboratory of Traffic Safety on Track of Ministry of Education, School of Traffic & Transportation Engineering, Central South University, Changsha, China, 410075
Email:2281055221@qq.com, yong_peng@csu.edu.cn

Abstract

Objective: This study proposes a planing style energy absorbing structure to improve the crashing performance of subway vehicles through experiment and numerical simulations. The structure consists of anti-creeper device, energy absorption tube, cutting knife and the clamp.

Method: In this paper, a finite element (FE) model of planing style energy absorbing anti-creeper device is created and validated by a full scaled experiment data. Then, based on the results of the validated simulation model, the influence of the designed parameters, which is the cutting depth (d) and the number of cutting knives (n) in the condition of the sum of the radius angle (RA) keep constant, on the impact performance is analyzed.

Results: it is found that the designed parameters have a apparent affluence on the cutting force and energy absorption(EA) of the proposed structure. In addition, the structure is found has prominent advantage in lowing the peak interface force.

Conclusions: The planing style energy absorbing structure has a nice impact performance and the design parameters have apparent influence on the crashworthiness of the structure.

Keywords: planing style energy-absorbing structure, numerical simulation, impact experiment

1. Introduction

The safety of passengers after railway collision accident has always been the hot spot of attention because of that the severe lose of casualties and property will be unbearable once the railway collision accident happened. For example, on July 12, 2008, a serious railway collision accident occurred in Los Angeles killed at least 26 people and more than 130 people injuries in the accident. Another similar collision happened in Wenzhou, China, on July 23, 2011, resulted in 40 people die and wounded at least 200 people. Thus, substantial investigations have been focused on the crashworthiness design and the optimization of energy absorption structure.

To date, many investigations have been putted to the crashworthiness design and optimization of energy absorption devices by use numerical simulation and experiment method. Thin-walled structures are widely used in civil engineering, shipbuilding, and other industries because of their low cost, high strength-weight ratio, progressively deform under an axial crushing load during crashworthiness analysis [1-2]. Based on the response surface method, Liu [3] optimized the cross-sectional dimensions of thin-walled structures to maximize the SEA and also presented efficient, simplified models that obtained optimum results of a certain accuracy. Nia and Hamedani [4] compared various section shapes of thin-walled tubes and concluded that the pyramidal and conical tubes can lower the peak force while the circular tube absorbs the most energy. Hosseinipour and Daneshi [5] found that grooves on the tubes can stabilize the deformation pattern to lower the deceleration pulse.

Furthermore, cellular material, as filler material for hollow tube, has an attractive mechanical properties to improve the crashworthiness and are widely used in automotive, military, and other industrial applications [6] and many studies[7-13] showed that aluminum foams have good energy absorption under both quasi-static and dynamic loading conditions. Paz et al [14] found that the honeycomb-filled tube showed an improved energy absorption over the hollow tube by performing tests with a hollow tube and a honeycomb filled tube. Regarding aluminum honeycomb sandwich panels, Paik et al [15] concluded that the aluminum honeycomb core among several core shapes and materials has excellent properties with consideration of weight savings and fabrication costs by a series of strength tests that carried out on aluminum honeycomb-cored sandwich panel specimen. Santosaa et al [16] found aluminum foam filling could give better crash behavior than aluminum honeycomb filling. While Bi et al [17] exhibited that the foam filled tube has a extraordinary larger crushing force than those of a hollow tube. Furthermore, a large undesirable initial peak force. Generally, there exists a large undesirable initial peak force, followed by fluctuation in the force-displacement curve[18]. Peng et al [19] focused on the study of the combination of thin-walled metal composite structures and aluminum honeycomb structures and founded that as the thickness or honeycomb yield strength increases, the initial peak force and average crashing force increases.

However, most studies have only focused on the parameter optimization of the thin-walled structure and the aluminum honeycomb structures or the composite structures. There are few studies put emphasis on the planing style energy absorbing structure, which works in the principle of that the plastic deformation of cutting chips, the avulsion of the metal tube, and the friction force between knives and curved metal will consume the impact energy. In this paper, an finite element model was established and validated by a full scaled impact experiment data in the same constraint conditions. The cutting depth and the number of cutting knives under the condition of that the the sum of the radius angle (RA) keep constant are set as the designed parameters. Based on the validated simulation model, the influence of the designed parameters on the crashworthiness performance was studied. In this work, several indicators including energy absorption(EA), peak interface force(F-max), the average cutting force (F-avg), cutting force efficiency(CFE) and stroke efficiency (SE) are defined as the crashworthiness indicators to systematically evaluate the crashworthiness of the planing style energy absorbing structure.

2. Methodology

2.1. Geometrical description

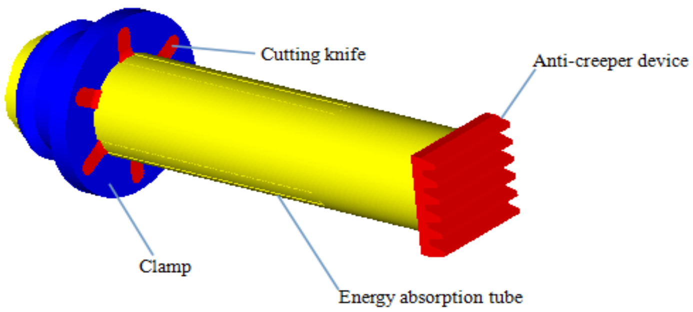

Fig.1. Planing style energy absorbing anti-climbing device

The energy absorbing device in this paper is usually fixed at the front end of the underframe of the subway. There are four parts in the structure.as is illustrated in Fig.1. The energy absorption tube,with outside diameter of 195 mm and inside diameter of 171 mm, consist of tube A(axis length of 694 mm) and tube B(axis length of 185 mm). The energy absorption tube can not only absorb energy when it is curved by the knives but also worked as a guide rail, which can guarantee that all the knives bear averaged force and the tube have a regular deformation pattern in the crash process. Sliding friction and shear slip deformation between cutting knife and metal layer have a significant contribution to the energy consumption. The knives are fixed on the clamp, which is weld on the underframe. Besides, the knives have a circular arc shape and the sum of radius angles of the knives are 127°. However, the anti-creeper device is fixed at the front-end of the tube A. In order to study the real situation in consideration of both energy absorbing structure and the train, full-scale experiment is conduct.In the real model , the energy absorbing device is weld on the vertical plate which is in the front of the impact trolley. Meanwhile, the tube A and B are fabricated in a horizontal line. Specifically, a pre-cutting is designed to decrease the first peak force and guide a regular deformation pattern.

2.2. Development of finite element (FE) model

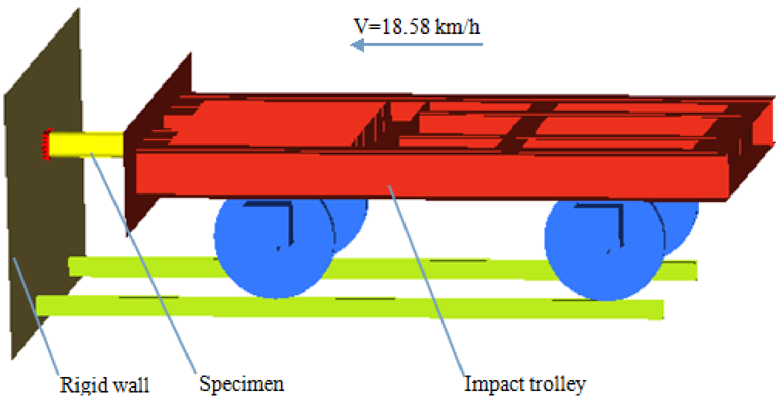

Fig.2. FE model and simulation conditions

With the development of computer technology and finite element theory, The finite element method has been widely approached to investigate the energy consumption process of metal energy absorbing devices. In this paper, the simulation model of collision process is developed in HyperMesh based upon the full scale physical experiment. Furthermore, LS-DYNA, an explicit nonlinear FE code is used to carry out the computing. As seen in Fig.2, the FE model mainly include the following parts: the energy absorbing structure, rigid wall and impact trolley. The energy absorbing structure is molded with solid element. In comparison, the Belytschko-Tsay shell element formulation is defined for the impact trolley.

For the consideration of both computational efficiency and the accuracy of the model,the mesh size 1-3mm and 8-12mm are selected for tube and the other area respectively. To avoid hourglass energy during the compute process this work choose the fourth hourglass control stiffness formula. The contact between energy absorbing device and rigid wall is defined by “AUTOMATIC_SURFACE_TO_SURFACE” contact algorithm. While the self-contact of curved chip is defined by “AUTOMATIC_SINGLE_SINGLE_SURFACE”. The contact between all the touched component are molded with a static friction coefficient of 0.25 and a dynamic friction coefficient of 0.3.

In the axial crush simulation model, there is a gravity acceleration of 9.818m/s^{2}and the whole model weights 24 tons, The energy absorbing structure which is fixed on the front end of the impact trolley impact onto the rigid wall at a speed of 18.58km/h.

2.2.1. Material model

The constitutive relationship of material reflects the changes of material property and plays an important role in the accuracy of the impact model. In this paper, the deformation of knives can be nearly ignored, thus, the knives are molded by hard alloy material while the other parts of energy absorbing structure are modeled by stainless steel Q235. Cowper-Symonds constitutive relationship model is selected because of its efficiency in react to the strain rate effect for a low strain rate condition[20]. The model adopts the factors associated with strain rate represent yield stress, as described by the following equation:

$$\sigma_y = \left[1 + \left(\frac{\dot{\varepsilon}}{C} \right)^{\frac{1}{P}} \right] \left(\sigma_0 + \beta E_\rho \varepsilon_\rho^{eff} \right) \tag{1}$$

$$E_\rho = E_{\tan} E / \left(E - E_{\tan} \right) \tag{2}$$

Where σ_y is the yield stress, σ_0 is the initial yield stress, $\dot{\varepsilon}$ is the strain rate, C and P are the strain rate parameters of the Cowper-Symonds constitutive relationship model, ε_ρ^{eff} is the effective plastic strain, and β is the hardening parameter, which varies from 0 to 1, E_ρ is the plastic hardening modulus, E is the modulus of elasticity, $E_{\tan}$ is the tangent modulus of plastic deformation[21]. In this work, the material parameters of tube and knives are shown in table 1.

Table 1. Material parameters of Q235 and hard alloy material

	Material	ρ /t • mm-3	E/Gpa	υ	σ_0 / Mpa	C/s-1	P	β	Failure strain
Tube	Q235	7.85×10-9	210	0.27	235	40	5	1	0.225
Knife	Hard alloy	1.48×10-8	608	0.3	-	-	-	-	-

2.3. Experimental set-up

In this work, a full scaled experiment, which can be seen in the Fig.3,is conducted in order to investigate the crash performance of the energy absorbing device during the crash process and validate the accuracy of the FE model for the further studies. An air cannon pulled the 24 t impact trolley to reached the designed velocity of 18.58km/h. Additionally, when the impact trolley reached the desired velocity, a preassembled automatic unhooking device was activated to separate the impact trolley from rope to prevent velocity from keeping increase. The velocity will be recorded by a infrared trigger equipment, while the high-speed camera captured the impact sequence of the energy absorption structure for the analysis of dynamic performance.

Fig.3. Experimental set-up

2.4. Structural crashworthiness criteria

A efficiency energy absorbing device is supposed to generate a controllable deformation pattern and meanwhile obtain maximum energy absorption and minimum cutting force during impact process. To quantitatively evaluate the crashworthiness performance of the structure, several design criteria, namely energy absorption(EA), peak interface force(F-max), the average cutting force(F-avg), cutting force efficiency(CFE) and stroke efficiency (SE) should be defined.

The energy absorption (EA) is a key indicator, which measures the energy absorption of the energy absorbing device and can be calculated by the following formula:

$$EA = \int_0^{\chi} F(\delta) d\delta \tag{3}$$

Where $F(\delta)$ is the instantaneous cutting force in the axial direction, which is a function of the displacements χ in the axial direction.

The peak interface force (F-max) is the maximum value of the $F(\delta)$, in the structure design process, a smaller value of it is desired. While the F_{avg} is also a key indicator for the energy absorption capacity of a structure, and defined as :

$$F_{avg} = \frac{EA}{\chi} \tag{4}$$

The cutting force efficiency(CFE) is defined as the ratio of the F_{avg} to $F_{\max}$. A larger value of CFE indicates a smooth impact process .

$$CFE = \frac{F_{avg}}{F_{\max}} \times 100\% \tag{5}$$

The stroke efficiency (SE) defined as the ratio between the effective strok-e length to the initial effective length of the energy absorption tube[22], that is 665mm in this paper.

3. Results

3.1 Validation of finite element(FE) model

In order to validate the accuracy of the developed FE model, a full scale experiment is conduct under the same boundary conditions with the simulation. As can be seen in the Fig.3, the experiment specimen has 6 knives and the cutting depth is 3mm. The results of experiment and simulation are represented in the force-time history curve and deformation series. Fig.4 and Fig.5 display the comparison of impact behaviors between the experiment and corresponding simulation, in terms of cutting force versus deformation time curve and deformation pattern respectively.

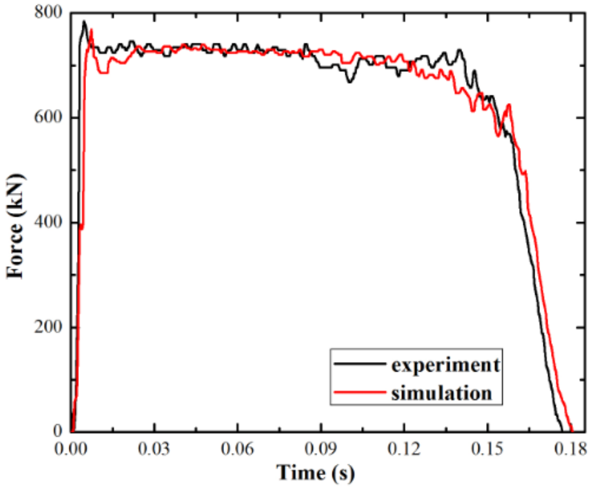

Fig.4. Experimental and numerical force-time force

As can be seen in the Fig.4, the curve tendency of experiment agree well with the corresponding simulation result. At about 5 ms, both of the curve reached at the peak interface force and the value is 780 kN and 768 kN for experiment and simulation. Then the force of simulation and experiment will stability in about 720kN and 725kN respectively. During the subsequent impact process, the force of experiment and simulation is essentially consistent and keeping stable but decreasing gradually. However, because of the complexity of the impact process and the test condition, the force versus time curve can not be absolutely consistent at each peak force point. For a better understanding, a detailed comparison of some key indicators are summarized in table 2.

Table 2. Comparison of critical indexes between experiment and simulation

Parameter	F_{max} (kN)	Cutting length (mm)	Duration time(ms)	F_{avg} (kN)	EA(kJ)
Simulation	768	395.5	181	706	279.1
Experiment	780	388.3	176	718	278.8
Error (%)	1.54	1.82	2.84	1.70	0.11

a

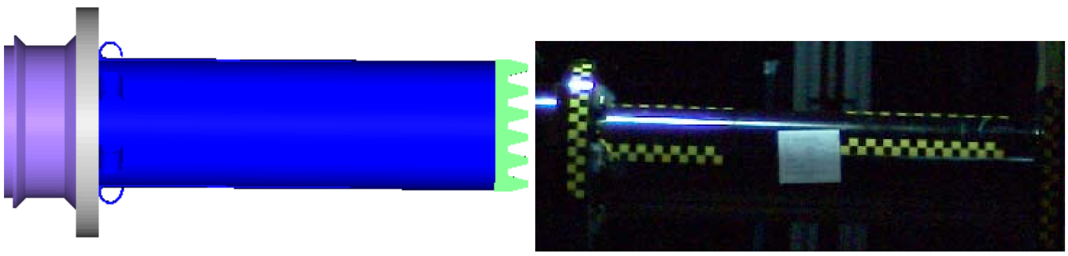

b

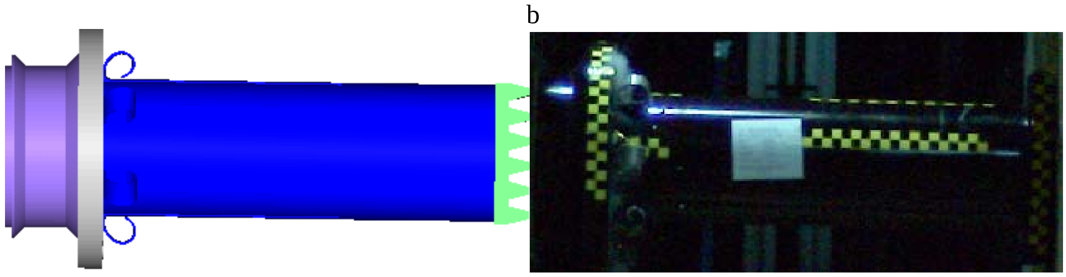

c

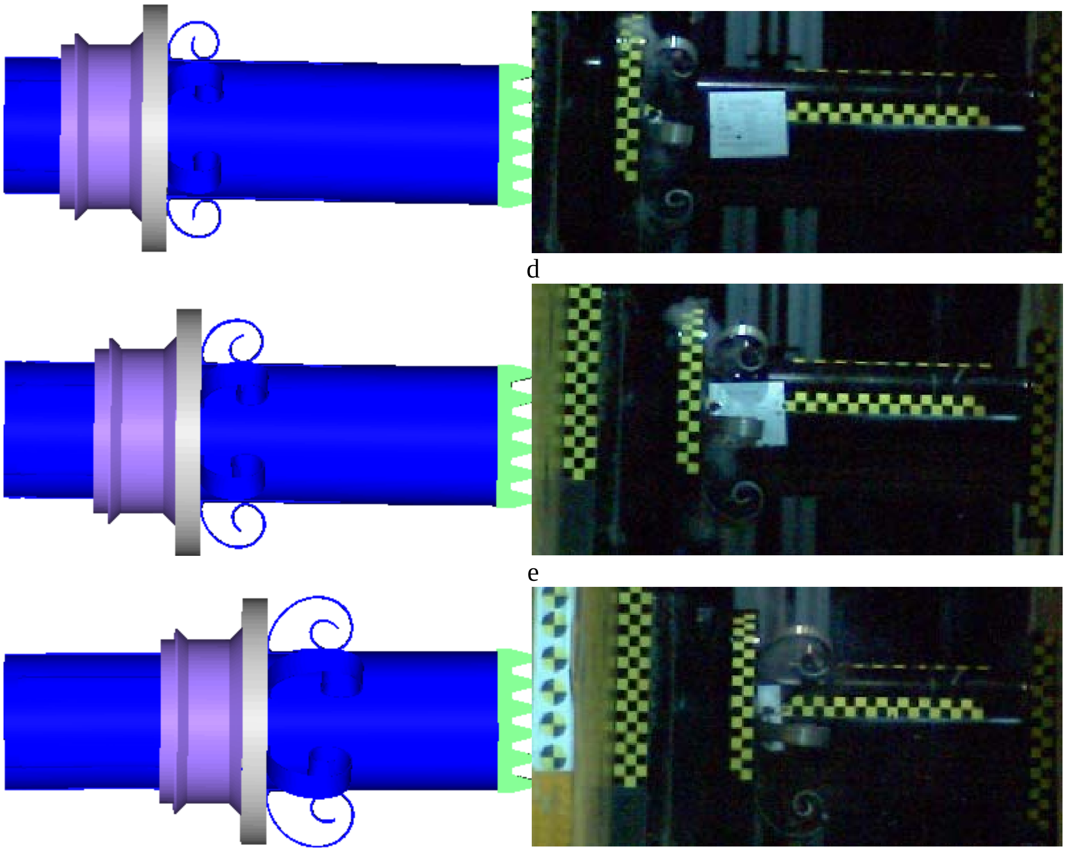

Fig.5. Comparison of deformation process between simulation and experiment results

Not only the impact response but also the deformation process should be considered in predict the impact results. The shape of deformation observed in the experiment agrees well with simulation results. In the Fig.5, there is the comparison of the time series of the side views of the energy absorbing structure between experiment and simulation. As can be seen, the deformation pattern of cutting chips, which is essentially the same, is just like a arc and the radian become smaller with impact process proceed. During the experiment, the image of deformation process is captured by the side set high speed camera with an ultra high rate of 1000 frames per second. At 0 ms, the anti-creeper device contact with the rigid wall initially. By the time of 165 ms, the cutting force is too small to cutting the tube sequentially. The whole impact process ended at about 175 ms when the system rebounded away from the rigid wall, which is also the time that the corresponds with the force duration time.

The force time history response curve and deformation pattern of simulation are compared to and found consistent with experiment date. It can be concluded that the FE model provide reasonable results and can be used in the next analysis.

3.2. Parametric study

In order to study the influence of the cutting depth and the number of the cutting knives on the impact performance of the energy absorbing devices, a parametric study is conducted in this paper. As shown in Table 3, 5 types of simulation are designed for the parametric analysis. Under the condition of the sum of the radius angle (RA) keep constant, we varied the number of the knives with 4, 6, and 8, respectively. Three types of cutting depth, 2mm, 3mm, and 4mm included in the simulations. The other constraints conditions are essentially the same with the tested FE model (type 6-3) except for the design parameter.

Table 3. Design of the FE model

Type	Number of knives / n	Cutting depth / d
6-2	6	2mm
6-3	6	3mm
6-4	6	4mm
4-3	4	3mm
8-3	8	3mm

3.2.1. Influence of the number of the cutting knives

In order to explore the effect of the number of cutting knives on the efficiency of the structure, the FE model of type 4-3 and type 8-3 were selected to compared with the type 6-3 in terms of the deformation pattern, force-time history curve, and the energy absorption.

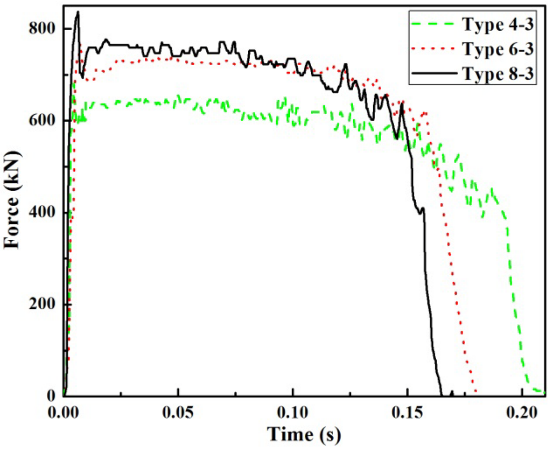

Fig.6. Force-time curve of different number of cutting knives

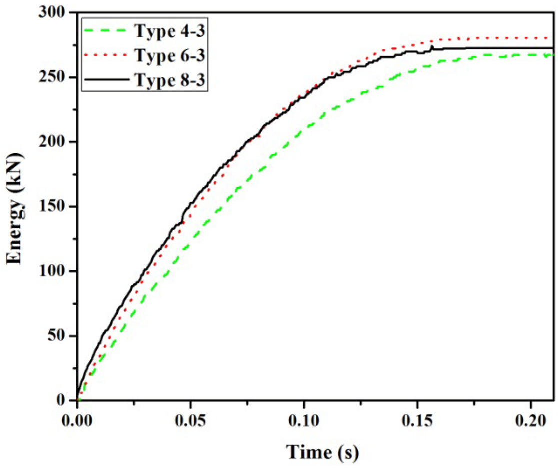

Fig.7. Internal energy-time curve of different number of cutting knives

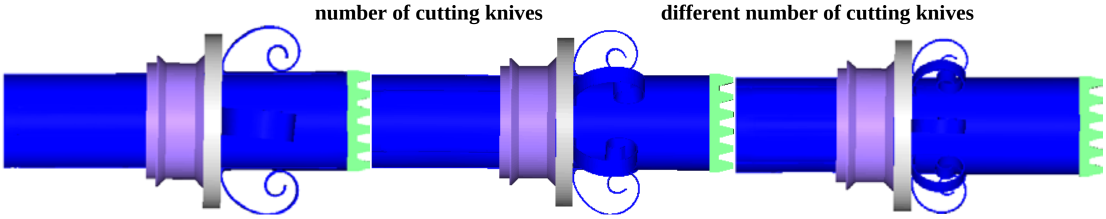

(a) Type 4-3 (b) Type6-3 (c) Type 8-3

Fig.8. Deformation results of different number of cutting knives

Table 4. Simulation results of different number of cutting knives

Type	F_{avg} (kN)	F_{max} (kN)	Cutting length (mm)	EA (kJ)	Duration time (ms)	CFE (%)
Type 4-3	616	677	432.2	266.2	205	91.0
Type 6-3	706	780	395.5	279.1	181	90.5
Type 8-3	741	832	366.4	271.4	165	89.1

Fig.8 shows the deformation pattern based on the different number of cutting knives. It is clear that the deformation of the cutting chips are essentially homogeneous, and the shape matches well with a arc, which explains that the curling force during the impact process is extraordinary smooth. Additionally, the curling radius of chip would keeping increase with the collision process proceed. However, referred to the length of curling chips, it can be concluded that, with the increase of the number of cutting knives, the impact distance will become shorter, which indicates that the cutting force will increase corresponding to the increase of designed parameter n.

From Fig.6, the trend of the force-time history force of type 6-3 is fairly similar to the type 4-3 and 8-3. As we can see, all of the model exhibit a relatively stable force followed by the initial peak interface force . The values of several key indicators are illustrate in the table 4. From both Fig.6 and Table 4, it is easy to be concluded that the type 4-3 model supports the minimum average force, peak interface force and the longest duration time. On the contrary, the average force and the initial peak force of the type 8-3 are the largest of the three model. Notably, the values of CFE varies from 0.89 to 0.91, which means that the planing style energy absorption structure can obtain a quite low deceleration pulse during the collision process.

Energy absorption is one of the most important criteria to study the crashworthiness of the device. Fig.7 illustrates the internal energy-time curve for the different number of knives. As can be seen, the internal energy increased as time goes by and keep a stable value at the end stage. Although the duration time of model 4-3 is the longest of the three model, the energy line of it is the lower than the other model because of the minimum cutting force. The type 8-3 model exhibit the maximum cutting force, and the energy line is greatest, however, it is exceeded the model 6-3 by the time of t=80 ms as a result of the shortest duration time and cutting length. The figure also shows that the slope of the energy line increased as the number of cutting knives increased.

3.2.2. Influence of the cutting depth

In addition to the number of cutting knives, the cutting depth can also affect the crash performance of the planing style energy absorbing structure. To explore the influence of the cutting depth, Type 6-2 and Type 6-4 simulation model are designed to compare with Type 6-3 model.

According to the deformation results exhibited in the Fig.11 ,all of the model showed regular cutting deformation mode, the crispate cutting chips generated sequentially with the impact process proceed. However, the compression distance is obviously different, Type 6-2 model experienced the largest distance and a successive decrease observed in the Type 6-3 model and Type 6-4 model.

Fig.9 exhibits the force versus time history curve of different cutting depth of the energy absorbing devices. All of the curves show a sharp initial force, however, combined with the table 5, the value of CFE varies from 0.85 to 0.91, which means the structure shows a prominent advantage in decreasing the initial peak force. After the peak force, the force line will be in a stable stage before the force become zero. As shown in the Fig.9, the model 6-4 bears the largest cutting force and the shortest duration time that is contrary to the model 6-2, which explains that with the cutting depth increased, the cutting force will increased while the duration time will decreased.

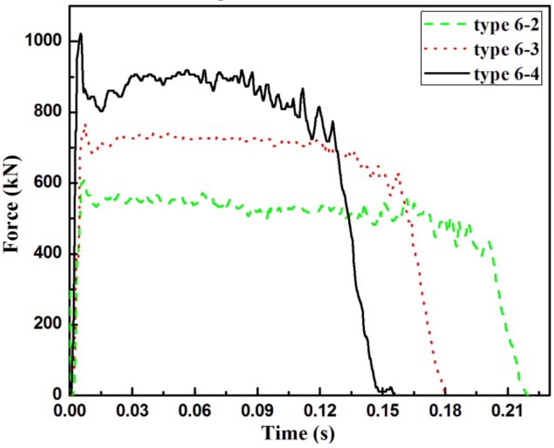

Fig.9. Force-time curve of different cutting depth

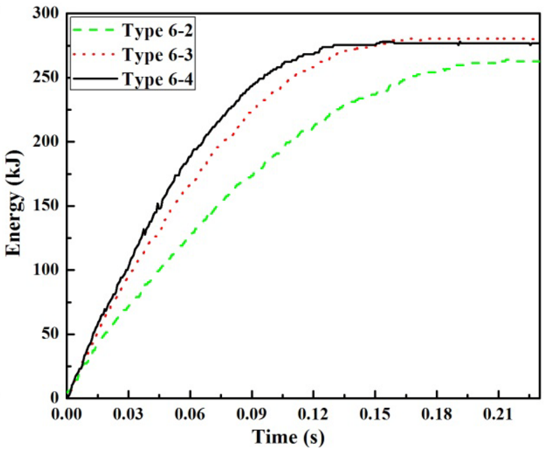

Fig.10. Internal energy-time curve of different cutting depth

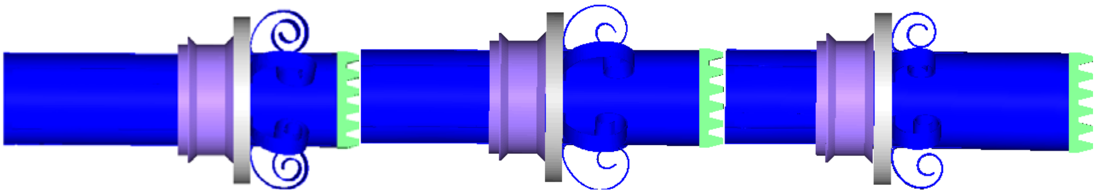

(a) Type 6-2 (b) Type 6-3 (c) Type 6-4

Fig.11. Deformation results of different cutting depth

Table 5. Simulation results of different cutting depth

Type	F_{avg} (kN)	F_{max} (kN)	Cutting length (mm)	EA (kJ)	Duration time (ms)	CFE %
Type 6-2	530	601	494.5	262.0	219	88.2
Type 6-3	706	780	395.5	279.1	181	90.5
Type6-4	865	1015	320.0	276.7	155	85.2

Fig.10 shows the internal energy-time curves of different cutting depth. It is obviously that, as the impact process progressed, all of the energy lines present a upward growth until arrive a maximum value. As can be seen, a thicker cutting chip correspond to a larger slope of the energy line, though not for the final energy absorption as a result of the duration time and cutting length will decreased as the cutting depth increased. That the type 6-3 model consume the most energy indicate a good energy absorption should comprehensive considerate both the cutting force and the cutting length.

4 Conclusions

To explore the the impact behaviors of planing style energy absorbing anti-climbing device, in this paper, the numerical model was created based on the non-linear finite element code LS-DYNA and validated by a full scaled experiment under the same constraint conditions. According to the validated FE model, the influence of the designed parameters, number of cutting knives and cutting depth, on the crashworthiness of the planning style energy absorbing anti-climbing device was analyzed.

The simulation results shows that the value of CFE varies from 0.85 to 0.91, which indicates that the planning style energy absorbing device showed a prominent advantage in lowing the initial peak force and the deceleration pulse.By comparing the simulation results of different parameters, it can be concluded that with the increase of cutting depth the cutting force will increase while the cutting length will decrease. In order to obtain the effective energy absorption, both the cutting force and the cutting length should be comprehensively considered. Similarly, the more number of cutting knives correspond to the larger cutting force. With a certain range of knife number, too many or too few cutting knives will decrease the energy absorption. However, a further systematically optimization study should be conducted for the optimal structural parameters of the planing style energy absorbing anti-climbing device.

Acknowledgments

The work was supported from the National Natural Science Foundation of China (51405517,U1334208) and the Natural Science Foundation of Hunan (2015JJ3155).

Reference

[1] A.A. Nia, J.H. Hamedani, Comparative analysis of energy absorption and deformations of thin walled tubes with various section geometries, Thin-WalledStruct. 48 (12) (2010) 946–954.

[2] H.S. Kim, T. Wierzbicki, Crush behavior of thin-walled prismatic columns under combined bending and compression, Comput. Struct. 79 (2001) 1417-1432.

[3] Y.C. Liu, Optimum design of straight thin-walled box section beams forcrashworthiness analysis, Finite Elem. Anal. Des. 44 (3) (2008) 139–147.

[4] S.J. Hou, Q. Li, S.Y. Long, X.J. Yang, W. Li, Design optimization of regular hexagonal thin-walled columns with crashworthiness criteria, Finite Elem. Anal.Des. 43 (6) (2007) 555–565.

[5] S.J. Hosseinipour, G.H. Daneshi, Energy absorbtion and mean crushing load ofthin-walled grooved tubes under axial compression, Thin-Walled Struct. 41(2003) 31–46.

[6] J. Banhart, Manufacture, characterisation and application of cellular metalsand metal foams, Progress in Material Science 46 (6) (2001) 559.

[7] T. Miyoshi, M. Itoh, T. Mukai, H. Kanahashi, H. Kohzu, S. Tanabe, K. Higashi,Enhancement of energy absorption in a closed-cell aluminum by themodification of cellular structures, Scripta Materialia 40 (1999) 1055.

[8] H. Kanahashi, T. Mukai, Y. Yamada, K. Shimojima, M. Mabuchi, T.G. Nieh, K.Higashi, Dynamic compression of an ultra-low density aluminum foam,Material Science and Engineering A 280 (2000) 349.

[9] A. Paul, U. Ramamurty, Strain rate sensitivity of a closed-cell aluminum foam,Material Science and Engineering A 281 (2000) 1.

[10] S.L. Lopatnikov, B.A. Gama, M.J. Haque, C. Krauthauser, J.W. Gillespie Jr, Highvelocity plate impact of metal foams, International Journal of ImpactEngineering 30 (2004) 421–445.

[11] S.L. Lopatnikov, B.A. Gama, M.J. haque, C. Krauthauser, J.W. Gillespie Jr, M.Guden, I.W. Hall, Dynamics of metal foam deformation during Taylorcylinder-Hopkinson bar impact experiment, Composite Structures 61(2003) 61–71.

[12] P.J. Tan, S.R. Reid, J.J. Harrigan, Z. Zou, S. Li, Dynamic compressive strengthproperties of aluminum foams. Part I—experimental data and observations,Journal of the Mechanics and Physics of Solids 53 (2005) 2174–2205.

[13] P.J. Tan, S.R. Reid, J.J. Harrigan, Z. Zou, S. Li, Dynamic compressive strengthproperties of aluminum foams. Part II—'shock' theory and comparison withexperimental data and numerical models, Journal of the Mechanics andPhysics of Solids 53 (2005) 2174–2205.

[14] J. Paz, J. Diaz, L. Romera, M. Costas, Crushing analysis and multi-objectivecrashworthiness optimization of GFRP honeycomb-filled energy absorptiondevices, Finite Elem. Anal. Des. 91 (2014) 30–39.

[15] J.K. Paik, A.K. Thayamballi, G.S. Kim, The strength characteristic of aluminum honeycomb sandwich panels, Thin-Walled Struct. 35 (3) (1999) 205-231.

[16] S. Santosa, T. Wierzbicki, Crash behavior of box columns filled with aluminum honeycomb or foam, Comput. Struct. 68 (4) (1998) 343-367.

[17] J. Bi, H.B. Fang, Q. Wang, X.C. Ren, Modeling and optimization of foam-filledthin-walled columns for crashworthiness designs, Finite Elem. Anal. Des. 46(2010) 698–709

[18] J. Song, Y. Chen, G.X. Lu, Axial crushing of thin-walled structures with origami patterns, Thin-Walled Stuct. 54 (2012) 65-71.

[19] Y. Peng, W. Y. Deng, P. Xu, S. G. Yao, Study on the collision performance of a composite energy-absorbing structure for subway vehicles, Thin-walled Struct. 94 (2015) 663-672.

[20] S.C. Xie, H. Zhou, Impact characteristics of a composite energy absorbingbearing structure for railway vehicles, Compos. Part B: Eng. 67 (2014)455–463

[21] M.H. Fatt, T. Wierzbicki, M. Moussouros, Rigid-plastic approximation for predicting plastic deformation of cylindrical shells subject to dynamic loading, Shock and Vibration Journal. 3 (3) (1996) 169-181.

[22] W.G. Chen, T. Wierzbicki, Relative merits of single-cell, muti-cell and foam-filled thin-walled structures in energy absorption, Thin-Walled Struct. 39 (4) (2001) 287-306.